

1 Supplementary information for: Closing the balance - on the role of
2 integrating biorefineries in the future energy system

3 Julia Granacher^{1*}, Rafael Castro-Amoedo¹, Jonas Schnidrig¹, François Maréchal¹

4 10th July 2023

5 ¹Industrial Process and Energy Systems Engineering group, École Polytechnique Fédérale de Lausanne,
6 Rue de l'Industrie 17, 1950 Sion, Switzerland;

7 *julia.granacher@epfl.ch

8 **Contents**

9	A Supplementary information on the superstructure model	2
10	A.1 Thermoechemical conversion pathways	2
11	A.2 Fuel cell and co-electrolysis	6
12	A.3 Carbon capture, mineralization, and geological sequestration	6
13	A.4 Residential district	8
14	A.5 Demands of residential district	11
15	B Supplementary information on parameter space and the solution synthesis	12
16	B.1 Mathematical formulation	12
17	B.2 Complexity reduction by means of time series aggregation	14
18	B.3 Parameter sampling and time-dependency	15
19	B.4 Country-specific data	18
20	C Supplementary information on the results	20
21	D Design references	20

22 A Supplementary information on the superstructure model

23 In the following, supplementary material on the characteristics of the superstructure is provided. Detailed
 24 descriptions of the considered superstructure for combined pulp and fuel production, including the Kraft
 25 pulp mill, thermochemical conversion pathways and fuel synthesis models are available in [1], the following
 26 provides a summary of the process model parameters.

Table 1: Kraft pulp mill.

	Unit	Value	References
Pulp mill			
Pulp production	adt/day	1000	[2]
Black liquor stream	kg/s for 1000 adt pulp/day	14.89	[2]
Bark stream	kW bark/adt pulp	33.5	[3]
Lime kiln and chemical recovery			[4, 5]
$T_{\text{calcination}}$	$^{\circ}\text{C}$	900	[4, 5]
T_{product}	$^{\circ}\text{C}$	300	[6]
Reburn specific heat	J/kg/K	989	[4]
CO ₂ specific heat	J/kg/K	919	[4]
Heat of calcination	kJ/kg	3270	[4]
Inerts specific heat	J/kg/K	1046	[4]
Availability	%	85	[6]
Dust loss	%	5	private data
Solid content	%	73.5	private data
Enthalpy of evaporation	kJ/kg	2439	[4]
Na ₂ CO ₃ in smelt	g/kg dry solids black liquor	278.3	[7]
Shell losses in kiln	% of heat input	15	[8]

27 A.1 Thermochemical conversion pathways

Table 2: Black liquor gasification.

	Unit	Value	References
Gasification of black liquor			
Hydrolysis			[9]
Lignin fraction in organic biomass	wt % _{DAF}	94	
H/C-ratio of lignin	mol _{DAF}	1.11	
O/C-ratio of lignin	mol _{DAF}	0.33	
Effective water content	wt%	93	
Decomposition of carboxylic salts			[10],[11]
Reactor yield	-	0.7	
Salt separator			[12]
Recovery of inorganic cooking chemicals	%	100	[13]
Organic losses in salt brine	%	10	[9]
Hydrothermal Gasification			[9]
Reactor temperature	°C	700	[14]
Reactor pressure	bar	250	[15]
Gas expander isentr. efficiency	-	0.8	[15]
Liquid expander isentr. efficiency	-	0.82	[15]
Pressure Swing adsorption (PSA)			[16]
Recovery	%	52	
Purity	mol%	99.996	
Number of beds	-	4	
Operating pressure	bar	30	[17]
Operating temperature	°C	25	[18]
Adsorbent		Activated carbon/zeolite	
Selexol and Pressure Swing adsorption			[9, 17, 19]
Pressure selexol/ PSA	bar	70/ 30	
Temperature selexol/ PSA	°C	25	
Recovery H ₂ selexol	%	100	
Recovery H ₂ PSA	%	80	
Number of beds PSA	-	6	
Purity	mol %	99.997	
COS hydrolysis			[20]
Temperature	°C	220	

Pressure	bar	depending on AGR unit
Warm-Temperature Syngas Desulfurization		[21, 22]
Temperature	°C	330
Pressure	bar	30

Table 3: Thermochemical conversion pathways of bark.

	Unit	Value	References
Pretreatment			[23–26]
Drying technology	-	Steam/air drying	
Moisture content after drying	%	10 (FT) / 20	
Gasification			[23–26]
Operating conditions (T,p), agent, steam to dry biomass ratio			
Directly heated entrained flow (ENF)	°C, bar, -,-	1350, 30, oxygen-steam, 0.6	
Directly heated circulating fluidized bed (CFB)	°C, bar, -,-	850,1, oxygen-steam, 0.6	
Indirectly heated fast internally circulating fluidized bed (FICFB)	°C, bar, -,-	850,1, oxygen-steam, 0.5	
Gas conditioning			[23–26]
Gas cleaning technology	-	cold/hot	
Gas cleaning temperature	°C	150 / 850	
Gas cleaning filter pressure drop	mbar	1000	
Gas cleaning flash temperature	°C	25	
water gas shift (WGS) temperature	°C	300	
CO ₂ removal	-	MEA	[27]
MEA heat requirements	MJ/kg CO ₂	3.3 (at 150°C, 20% recoverable)	
MEA electricity requirements	kJ/kg CO ₂	25	
Fuel synthesis			[23–26]
Operating conditions			
Fischer-Tropsch (FT) synthesis pressure, temperature	bar, °C	25,220	
dimethyl ether (DME) synthesis pressure, temperature	bar, °C	50,277	
methanol synthesis pressure, temperature	bar, °C	85,315	
synthetic natural gas (SNG) synthesis pressure, temperature	bar, °C	5,327	
Technology and catalyst			

FT synthesis	Multi tubular fixed bed reactor, Co/Zr/SiO ₂
DME synthesis	Slurry phase reactor , ACZ, HZSM-5
Methanol synthesis	Multi-stage fixed bed reactor , Cu/ZnO/Al ₂ O ₃
SNG synthesis	Internally cooled fluidized bed reactor , NiAl ₂ O ₃
<hr/>	
Upgrading	[23–26]
<hr/>	
FT upgrading	Private data
DME upgrading	Flash distillation
Methanol upgrading	Flash distillation
SNG upgrading	Membranes, PSA
<hr/>	
Fuel specifications	[23–26]
<hr/>	
FT specification, temperature, pressure	-, °C , bar Liquid fuels, 25, 1
DME specification, temperature, pressure	-, °C , bar 99.8 vol%, 25, 1
Methanol specification, temperature, pressure	-, °C , bar 99.4 vol%, 25, 1
SNG specification, temperature, pressure	-, °C , bar 96 vol%, 25, 50
<hr/>	

28 A.2 Fuel cell and co-electrolysis

29 Table 4 summarizes the key modeling assumptions for the electrolysis and fuel cell models added to the
30 superstructure.

31 A.3 Carbon capture, mineralization, and geological sequestration

32 The models for direct and indirect mineralization are adapted from Ostovari, Sternberg and Bardow [31]
33 and Spínola et al. [32], considering serpentine as possible feedstock to complement residues from the mill.
34 Hereafter, the main process modeling assumptions are summarized; details on the adapted simulation
35 models can be found in [33].

Table 4: SOEC/SOFC units.

	Unit	Value	Reference
Alkaline electrolysis			
Water in	kg/s	0.080	[28]
Hydrogen out	kg/s	0.069	[28]
Oxygen out	kg/h	0.170	[28]
Electricity in	kWh	1000	[28]
System efficiency	kWe/kg H ₂	52	[28]
Solide oxide Co-electrolysis			[29]
Water inlet	kg/s	1.533	
CO ₂ input	kg/s	2.64	
Syngas produced	kg/s	3.011	
Oxygen co-produced	kg/s	1.162	
Electricity input	kW	18336	
Solide oxide fuel cell			[30]
F ^{min}	kWe	250	
CH ₄ in	kg/s	1	
CO ₂ out	kg/s	2.75	
η^{elec}	%	75	

Table 5: Direct mineralization.

	Unit	Value	Reference
Grinding and magnetic separation			[31, 34]
Serpentine in	t	2.3	
Electricity demand	kWh	190	
Magnetic material out	t	0.2	
Carbonation reactor and postprocessing			[31, 34]
Operating temperature	°C	155	
Operating pressure	bar	140	
MgCO ₃ out	t	1.9	
SiO ₂ out	t	0.9	
Solvent recovery rate	%	90	

Table 6: Indirect mineralization.

	Unit	Value	Reference
Grinding and Phase 1 reactor: mineral extraction			[31, 34]
Serpentine in	t	3.9	
Electricity demand	kWh	63	
Ammonium sulfate makeup	t	0.3	
Phase 2 reactor: hydroxide formation			[31, 34]
Operating temperature	°C	50	
Operating pressure	bar	0.5	
Phase 3 reactor: carbonation and postprocessing			[31, 34]
Operating temperature	°C	300	
Operating pressure	bar	25	
MgCO ₃ out	t	2	

36 Carbon capture is modeled as a blackbox model of monoethanolamine (MEA) with specific heat and
37 electricity requirements and performance indicators from Heyne and Harvey [27]. For geological sequest-
38 ration, compression of CO₂ to high-pressure levels for transportation is required. The costs for transport
39 and storage are provided in Table 14. Sequestration and MEA modeling assumptions are summarized in
40 Table 7.

Table 7: Carbon capture and sequestration.

	Unit	Value	Reference
CO₂ capture technology			[27]
Electricity demand	kJ/kg CO ₂	25	
Heat demand, temperature	MJ/kg CO ₂ , °C	3.3, 150 ^a	
CO ₂ /water removal rate	%	95	
Sequestration			
Pressure	bar	60	[35]

^a20% of heat are recoverable between 90 and 40°C [27].

41 A.4 Residential district

42 Table 8 provides information about the heating technology units and the photovoltaic units. The invest-
43 ment costs for the installation of the district heating network (DHN) are calculated using the approach
44 provided in [36] with specific cost data from Belfiore [37], and average heat loss assumptions from Masatin,

45 Latõšev and Volkova [38]. Two types of district heating networks are considered in the superstructure, a
46 fourth generation, medium-temperature water district heating network, operating at supply and return
47 temperatures of 60 °C and 30 °C, respectively, as well as an innovative fifth-generation district heating
48 network, operating on CO₂ as the working fluid with supply and return temperatures of 15 °C and 13 °C.
49 Both DHN models are adapted from RA Suciu [36].
50 For providing the heat at the required temperature levels for space heating and domestic hot water
51 demands, heat pumps can be installed at the district level; the models are adapted from RA Suciu [36]
52 and Henchoz et al. [39]. The network is balanced using a central plant that exchanges heat with the
53 pulp mill and can provide additional heat to the DHN by heat pumping (CO₂ network, heat pump
54 model adapted from RA Suciu [36]) or a conventional boiler operation (water network, boiler model
55 adapted from [40]). The residential district model is limited by simplifications regarding temperatures of
56 the demands and their dependency on external conditions. For modeling transportation efficiencies, the
57 assumption in Table 9 are used. Table 10 provides the energy content of the fuels used for the analysis of
58 the transportation demands, further elaborated the main article.

Table 8: District model characteristics.

	Unit	Value	Reference
District heating network			[30, 39, 41]
Water network, T^{supply} , T^{return}	°C	60, 30	
CO ₂ network T^{supply} , T^{return}	°C	15, 13	
CO ₂ network pressure	bar	50	
Conventional heating system			
Fuel split in commune heating	%	20/40/40 (gas/oil/other)	[42]
Efficiency gas boiler	%	95	[43]
Photovoltaic			[36, 44]
T^{a}	°C	15	
T^{ref}	°C	25	
U^{glass}	W/m ²	29.1	
Solar irradiation through PV glass f^{glass}	-	0.9	
Efficiency $\eta^{\text{pv,ref}}$	-	0.14	
$\eta^{\text{pv,variation}}$	-	0.001	
Electricity provision ^a , $E^{-\text{PV}}$	kW	1.66	

^afor reference area of A=100 m² and irradiation I=100 W/m².

Table 9: Efficiency of transport mediums.

Modelling assumptions	Unit	Value	Reference
in 2019			[45]
Fuel-powered car	MJ/pkm	1.78	
Electric car	kWh/vkm	0.17	[46]
Bus	MJ/pkm	1.01	
Freight	MJ/tkm	2.74	
in 2030 ^a			
Fuel-powered car	MJ/pkm	0.98	
Electric car	kWh/vkm	0.17	[46]
Bus	MJ/pkm	0.56	
Freight	MJ/tkm	1.51	

^aassuming linear efficiency improvement from [47].

Table 10: lower heating value (LHV) and exergy of products and fuels^a.

Product	LHV [MJ/kg]	Exergy [MJ/kg]
FT fuel	44.81	47.94
Methanol	19.83	21.22
DME	28.83	30.84
SNG	47.89	52.12
Hydrogen	119.70	116.50
Pulp	8.15	9.21
Diesel	42.61	NA
Gasoline	43.45	NA
Nat. gas	50.02	NA

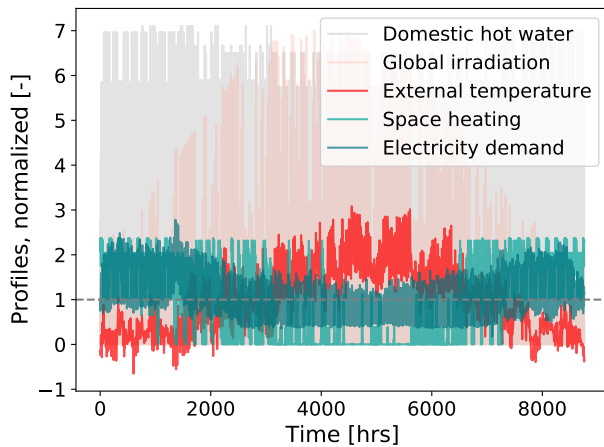
^aLHV based on flowsheeting results, exergy calculated with factors provided in [48].

59 A.5 Demands of residential district

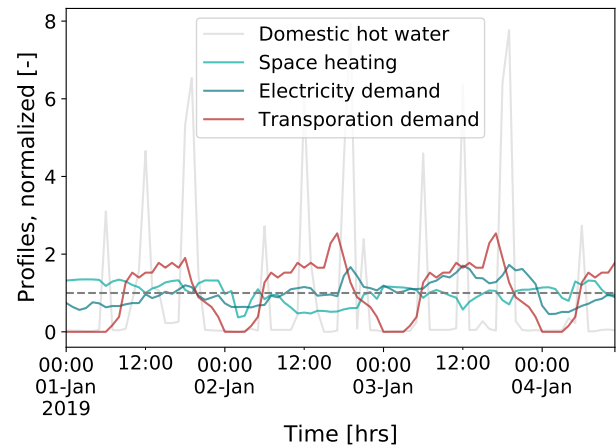
60 The average transportation demand is summarized in Table 11, information on the heating and electricity
 61 demands of the district, as well as the weather data is provided in Table 12 for average annual data. In
 62 Figure 1, samples of the hourly demand profiles included in the model are presented and normalized on
 63 the respective annual averages.

Table 11: Shares of passenger vehicles in France for 2019 and 2030.

Value	Unit	Commodity	Reference
2019			[49]
27	%	Gasoline	
71	%	Diesel	
2	%	Electricity and others	
2030			[50]
16	%	Gasoline	
24	%	Diesel	
60	%	Electricity and others	



(a) Hourly profile, one year



(b) Hourly profile, four days

Figure 1: Hourly district demands and weather data profiles for one year, adapted from Middelhauve [51], PM Stadler [52] and Cedric Terrier, Luise Middelhauve and François Maréchal [53].

Table 12: District demands and weather data.

	Unit	Value	Reference
Size and demands^a			[51, 52]
Reference size district	capita	568	
Scaling factor district	-	300/150 ^b	
Annual average demands per capita^a			
Domestic hot water demands	kWh	630	[51, 52]
Space heating demand	kWh	4080	[51, 52]
Electricity demand	kWh	1200	[51, 52]
Personal transport demand	pkm	10800	[53]
Freight transport demand	tkm/yr	4300	[54]
Public transport demand	pkm/yr	4500	[49]
Annual average weather data^a			[51, 52]
Global irradiation G^I	W/m ²	135	
External temperature T^{ext}	°C	10.4	

^ademands and weather data are given as annual average; in the model, data for hourly resolution is included from the respective references, ^byields a city size of 170000 and 85000 inhabitants.

64 B Supplementary information on parameter space and the solution 65 synthesis

66 B.1 Mathematical formulation and heat exchange characteristics of superstructure 67 optimization problem

68 The mathematical formulation of the superstructure and optimization in the lower level is adapted from
69 [55, 56], it has also been applied and described in detail in previous studies, such as [1, 57]. The main
70 aspects are summarized hereafter; for more details, the interested reader may consult the cited references.
71 For each unit u in the system, energy and mass flow models are built to describe the conversion in the
72 unit regarding streams, physical properties, mass, and energy balances, and to obtain the characteristics
73 of the interfaces offered for integration with other units. Presuming a set of possible units \mathbf{U} and a set
74 of possible system states \mathbf{T} , binary decision variables y_u^{use} and $y_{u,t}^{\text{use}}$ define whether a unit is installed and
75 whether it is used in timestep t . Continuous decision variables f_u^{mult} and $f_{u,t}^{\text{mult}}$ describe the size of the
76 installed unit and the level of usage at which it is operated in each period t . Continuous variables f_u^{mult} are
77 constrained by parameterized upper and lower bounds $F_u^{\text{min/max}}$. Similarly, the binary decision variables
78 y_u^{use} and $y_{u,t}^{\text{use}}$ are limited by Y_u that determines whether a unit is considered for the generation of results.

79 In the superstructure model, these variables are related to each other by the set of Equations 1- 3.

$$F_u^{\min} \cdot y_u^{\text{use}} \leq f_u^{\text{mult}} \leq F_u^{\max} \cdot y_u^{\text{use}} \quad \forall u \in \mathbf{U} \quad (1)$$

$$F_u^{\min} \cdot y_{u,t}^{\text{use}} \leq f_{u,t}^{\text{mult}} \leq F_u^{\max} \cdot y_{u,t}^{\text{use}} \quad \forall u \in \mathbf{U}, t \in \mathbf{T} \quad (2)$$

$$Y_u \geq y_u^{\text{use}} \geq y_{u,t}^{\text{use}} \quad \forall u \in \mathbf{U}, t \in \mathbf{T} \quad (3)$$

80 Requirements for each resource are satisfied by internal production and imports (Equation 4). The overall
 81 resource balance ensures that import, export, production, and consumption are balanced in the system, as
 82 formulated in Equation 5. $\dot{m}_{re,u,t}^+$ and $\dot{m}_{re,u,t}^-$ define the reference mass flow rate of resource re consumed
 83 (+) and provided (-), respectively, in unit u at timestep t . For each unit, the mass balance of streams
 84 entering and leaving in a timestep t needs to be closed (Equation 6). It needs to be noted that for clarity
 85 of the following mass balance formulation, both in and outgoing streams are labeled as resource, with
 86 the respective sign (+/-) indicating the direction. In the main text of this thesis, outgoing resources
 87 might be referred to as services (se) provided by the mill. More detailed information on the mathematical
 88 formulation of the superstructure optimization problem applied in this thesis is provided in [56].

$$\sum_u f_{u,t}^{\text{mult}} \cdot \dot{m}_{re,u,t}^- + \dot{M}_{re,t}^- - \sum_u f_{u,t}^{\text{mult}} \cdot \dot{m}_{re,u,t}^+ \geq 0, \quad \forall re \in \mathbf{RE}, \forall t \in \mathbf{T} \quad (4)$$

$$\sum_u f_{u,t}^{\text{mult}} \cdot \dot{m}_{re,u,t}^+ + \dot{M}_{re,t}^+ - \dot{M}_{re,t}^- - \sum_u f_{u,t}^{\text{mult}} \cdot \dot{m}_{re,u,t}^- = 0, \quad \forall re \in \mathbf{RE}, \forall t \in \mathbf{T} \quad (5)$$

$$\sum_{re} f_{u,t}^{\text{mult}} \cdot (\dot{m}_{re,u,t}^+ - \dot{m}_{re,u,t}^-) = 0, \quad \forall u \in \mathbf{U}, \forall t \in \mathbf{T} \quad (6)$$

89 All units are connected to a utility system, enabling the energy demand and supply profile of each unit
 90 to be satisfied, considering their respective temperature-enthalpy profiles. Minimum energy requirements
 91 are calculated applying the Pinch analysis and heat recovery approach presented by Marechal and Kal-
 92 itventzeff [58], based on the work of Linnhoff and Hindmarsh [59]. The list of all stream inlet and outlet
 93 temperatures is extracted and ordered to generate the set of temperature intervals \mathbf{K} of the size N^k [56].
 94 The energy balance is closed in each temperature interval k (Equation 7), and residual heat ($\dot{R}_{t,k}$) flows
 95 from higher to lower temperature levels. Following thermodynamic feasibility, cascaded heat flows are
 96 positive, while values in both the first and the last interval are zero (Equation 8). $\dot{q}_{u,t,k}$ represents the
 97 reference heat load for unit u in timestep t and temperature interval k [55].

$$\forall k \in \mathbf{K}$$

$$\sum_u \dot{q}_{u,t,k} \cdot f_{u,t}^{\text{mult}} + \dot{R}_{t,k+1} - \dot{R}_{t,k} = 0 \quad \forall t \in \mathbf{T} \quad (7)$$

$$\dot{R}_{t,k} \geq 0, \quad \dot{R}_{t,1} = \dot{R}_{t,N^k+1} = 0 \quad \forall t \in \mathbf{T} \quad (8)$$

98 In this work, the described mixed integer linear programming (MILP) formulation is further enhanced
 99 by simultaneous optimization of water and energy developed by Kermani et al. [60], where the thermal
 100 characteristics of water streams are considered for heat integration.

101 Within the mathematical formulation of the optimization problem in the lower-level framework, the energy
 102 and process models relevant to the superstructure are organized in so-called clusters. Clusters are defined
 103 as entities that can exchange resources freely among each other, but heat can only be exchanged between
 104 the different clusters by means of hot water loops or evaporation and condensation of water in the steam
 105 network [2]. Thus, per cluster, the heat cascade is defined, as described in Section B.1. Table 13 displays
 106 the organization of process units in different clusters for the analyzed system of combined pulp and fuel
 107 production, adapted from [2] and enhanced for considering fuel production.

Table 13: Cluster structure in lower-level optimization problem and included process units.

Cluster digester	Cluster recovery boiler	Cluster fuel production
Washing	Evaporator	Methanol synthesis
Digester	Recovery boiler	DME synthesis
Recausticizer	Biomass boiler	SNG production
		FT fuel synthesis
		Hydrothermal gasification
		Electrolysis
Cluster pulp machine		
Pulp machine		
Bleaching		

108 B.2 Complexity reduction by means of time series aggregation

109 Time series aggregation (TSA) methods have gained remarkable significance in the modeling and design
 110 of a wide range of energy system applications where seasonal, daily, or hourly variations in demand,
 111 supply, or parameter spaces are of importance. A comprehensive review is provided by Hoffmann et al.

112 [61], investigating TSA methods for modeling energy systems. Schütz et al. [62] compare aggregation
 113 methods based on their performance; it was found that k-medoids is most reliable when approximating
 114 costs of systems by means of TSA, which is also confirmed by Hoffmann et al. [61].

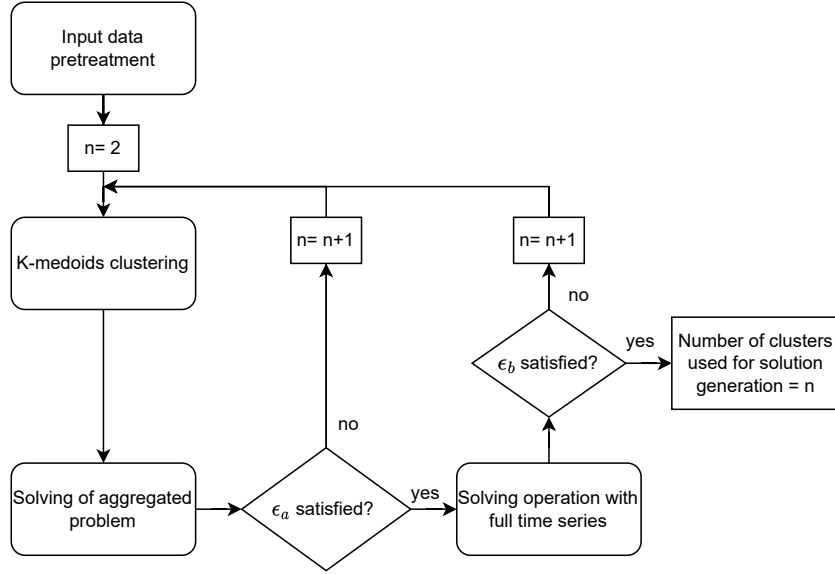


Figure 2: Proposed algorithm for determining the required number of clusters, adapted from Middelhaue et al. [63], Baumgärtner et al. [64] and Bahl et al. [65].

115 For determining the required number of clusters for analyzing the above-described superstructure ad-
 116 equately, a systematic method for bounding the error of the aggregation in the objective function is
 117 followed, as proposed by Baumgärtner et al. [64] and Bahl et al. [65] and further developed by Middel-
 118 haue et al. [63]. In each iteration of the incremental increase of TSA resolution, an upper and lower
 119 bound of the objectives are evaluated until a convergence criterion on the gap is met. The lower bound
 120 is derived from solving the relaxed problem, whereas the upper bound is defined as the solution of the
 121 operating problem in consideration of the complete time series and fixed unit sizes given by the relaxed
 122 solution [63–65]. Another convergence criterion is considered, in which the relaxed solution of a proposed
 123 number of clusters n is compared to the previous solution for $n - 1$ clusters. Only when a defined con-
 124 vergence criterion is reached, the operating problem is evaluated for the full-time series, fixing the unit
 125 decisions to the findings of the relaxed solution. The procedure for TSA is displayed in Figure 2.

126 B.3 Parameter sampling and time-dependency

127 For the consumed resources $re \in RE$ and provided services $se \in SE$, the nominal prices displayed in Table
 128 14 are included. Impact factors are taken from the Ecoinvent database, version 3.6 [66]. As mentioned

129 in the main article, samples are drawn twice from the parameter space, once for solution generation and
 130 once during solution exploration. For sampling when generating and exploring solutions, latin hypercube
 131 sampling (LHS) is applied for all parameters that are not assumed to be time-dependent. Table 15 gives
 132 an overview of the parameter variations considered in both sampling steps, not including time-dependent
 parameters such as electricity and fuel prices as well as the impact factors of electricity.

Table 14: Nominal values of key economic parameters considered in solution generation and exploration.

Parameters	Unit	Value	Reference
Interest rate	%	6	
Expected lifetime	years	20	
Wood price	USD/kg	0.093	[67]
Pulp price	USD/kg.	0.882	[68]
Electricity price ^a	USD kWh	0.105	[69]
Natural gas price	USD/kWh	0.026	[70]
FT price	USD/kg	-1.108	[71]
Methanol price	USD/kg	-0.390	[72]
DME price	USD/kg	-0.470	[73]
SNG price	USD/kWh	-0.075	[74]
H ₂ price	USD/kg	-2.500	[75]
Quicklime price	USD/kg	0.117	[76]
Freshwater price	USD/kg	0.0012	[77]
Landfill price	USD/kg	0.0013	[78]
CO ₂ sequestration: transport	USD/kg/250 km	4	[79]
CO ₂ sequestration: storage	USD/kg	11	[80]
Waste heat to district heating	USD/kWh	0.075	[81]
Diesel price ^b	USD/l	1.439	[82]
Gasoline price ^b	USD/l	1.515	[82]
Residential heating mix ^c	USD/kWh	0.0689	[36]

^aannual mean, variation with electricity price from [83], ^bannual mean, variation from WTI crude oil price from [84], ^ccurrent energy mix for heating and cost adapted from [36].

133
 134 For the time-dependency of energy commodities, the historical behavior of natural gas, electricity, and
 135 crude oil is considered. In the superstructure model, it is assumed that SNG prices follow trends of natural
 136 gas, whereas prices of liquid fuels follow the crude oil prices [86]. Annual means and the references for
 137 time-dependent economic data are provided in Table 14.

138 For including the time-dependent variation in the superstructure model for solution generation, the avail-
 139 able historical, time-dependent data is varied by two parameters: one that shifts the observed data either
 140 up or down and one that adds noise to the observed data points. The noise added follows a normal
 141 distribution with the standard deviation equaling half of the observed standard deviation in the historical

Table 15: Sampling characteristics of parameter space.

Parameter	Description	Variation ^a
$p^{\text{un}}(u)$	Normalized variation of investment cost of unit $u \in U^*$, $U^* =$ hydrolysis, salt separator, hydrothermal gasification, sulfur removal, CO ₂ removal	± 50
$p^{\text{un}}(u)$	Normalized variation of investment cost of unit $u \in U$, $U =$ electrolysis, co-electrolysis, brine electrolysis, dry biomass pretreatment, gasification, gas conditioning, fuel synthesis reactors (FT, MeOH, DME), SNG synthesis, storage tanks, PV, DHN, mineralization	± 20 [85]
$i^{\text{un}}(r)$	Normalized variation of impact of resource $r \in r$, except for electricity	± 20
$r^{\text{un}}(r)$	Normalized variation of market price of resource $r \in r$, except for electricity, natural gas, SNG and biofuels ^b	± 20

^aall parameters sampled with Latin Hypercube Sampling during solution generation and uniformly distributed for solution exploration. Parameters for which time-dependency is acknowledged are not displayed, ^bSNG, natural gas are considered to follow natural gas trends, biofuels are considered to follow crude oil prices.

142 data. The newly-obtained data is clustered based on the required number of clusters determined by TSA
143 and used as input for each formulated problem solved by the lower-level framework.
144 To ensure realistic data points are used for result generation, a literature review on correlations between
145 electricity, crude oil, and natural gas prices is conducted. Historically, natural gas and refined petroleum
146 products have been used as close substitutes in power generation and industry, leading to natural gas prices
147 tracking the prices of crude oil [87]. A strategic statistical analysis of the integrated energy market in
148 Europe is addressed by Bencivenga, Sargenti and D’Ecclesia [87], investigating the short-run relationship
149 between oil, natural gas, and electricity in the European energy markets, and identifying possible long-run
150 equilibrium relationships. Correlation analysis presented itself as non-effective due to the non-stationarity
151 of the data, but cointegration was able to detect a relationship between the individual commodities [87].
152 In 2014, a report requested by the European Parliament was released, investigating the dependencies in
153 the European energy market [88]. Electricity prices tend to vary considerably throughout Europe and
154 generally show a moderate correlation to oil price developments. Different Merit-order curves in different
155 countries lead to different electricity prices, and market integration into a single electricity market in
156 Europe has not yet been fully achieved [88]. Generally, oil product prices such as diesel and gasoline are
157 strongly related to crude oil prices because of the high share of feed-stock costs in their production [88].
158 The main pathway of high oil prices being translated into gas and electricity prices was originally induced
159 by the still dominant practice of indexing gas prices to oil prices, prevalent in most gas supply contracts

160 in Europe. It was found that even though gas and oil suppliers share common fundamental price drivers,
 161 if oil indexation is absent, gas and oil prices are often decoupled [88]. Recently, an increasing share of
 162 studies has addressed the inter-dependencies of actors in the energy market, especially encouraged by the
 163 increasing price volatility in the energy commodity markets, addressing risk management in the financial
 164 sector and the increasing interest in clean energy technology [89–91].

165 To acknowledge both time-dependent price and impact variation and inter-dependencies between com-
 166 modity prices in this study, the covariance of electricity prices regarding oil, natural gas prices, and
 167 environmental impact are calculated for different temporal resolutions. Between the electricity price and
 168 the impact, a positive correlation can be observed, meaning that more expensive electricity can be asso-
 169 ciated with a higher impact. For the oil and natural gas prices, no strong correlation is observed, even
 170 though both are mainly driven by the same components [86]. Reasons for this might be the different
 171 time-resolution of the obtained data, as well as the much more dynamic character of the electricity price
 172 that makes observations on correlation on an hourly basis challenging. Daily and biannual data reveal
 173 higher correlations, but since the data set used in this study is supposed to represent typical hours, this
 174 information is not adequate to draw conclusions.

175 Therefore, a ratio-based approach is applied instead of relying on the covariance, where oil and natural
 176 gas prices are sampled as previously described. A sample is accepted if the ratios between electricity
 177 price, gas price, and oil price are within the observed proportions in the historical data set. Obtained
 178 samples are then used to scale the energy prices included in the superstructure model. The price for SNG
 179 and natural gas is scaled with the sampled data for natural gas, liquid fuel prices with the crude oil price,
 180 and electricity prices with the electricity price sample. The applied ratios for acceptance are displayed in
 181 Table 16.

Table 16: Accepted ratios for sampling commodity prices, based on historical normalized prices.

Ratios [%]	Electricity price	Oil price	Natural gas price
Electricity price	1	40-800	90-120
Oil price	-	1	60-115
Natural gas price	-	-	1

182 B.4 Country-specific data

183 Country-specific data used to extrapolate the analysis to the European level is provided in Table 17.

Table 17: Country-level data to scale results to European level^a.

Country	M ^{pulp-}	c ^{nat.gas}	c ^{gasoline}	c ^{diesel}	c ^{elec} [2019]	e ^{t,elec} [2019]	c ^{elec,*b}	e ^{t,elec,*b}	Inh. country	Emi ^{country}
Unit	kt	EUR/kWh	EUR/l	EUR/l	EUR/kWh	g CO _{2-eq} /kWh	EUR/kWh	g CO _{2-eq} /kWh	Mio. capita	Mio t CO _{2-eq}
Reference	[92]	[70]	[82]	[82]	[69]	[83]	[93]	[93]	[94]	[95]
Belgium	1025	0.02	1.41	1.32	0.08	214.17	0.28	152.16	11.56	106.43
Bulgaria	242	0.03	1.09	1.11	0.09	281.40	0.15	40.94	6.92	49.19
Czechia	557	0.03	1.24	1.24	0.07	763.99	0.19	55.66	10.72	113.34
Germany	2326	0.03	1.43	1.27	0.08	431.31	0.18	54.86	83.20	728.74
Estonia	222	0.03	1.33	1.32	0.08	561.79	0.18	40.24	1.33	11.56
Spain	1456	0.03	1.29	1.22	0.09	224.69	0.14	37.48	47.37	274.74
France	1626	0.03	1.50	1.44	0.08	69.10	0.15	37.19	68.10	392.96
Croatia	47	0.03	1.34	1.32	0.09	346.72	0.13	34.91	4.04	23.76
Italy	334	0.03	1.57	1.48	0.09	383.81	0.13	34.91	59.33	381.25
Hungary	28	0.03	1.17	1.23	0.09	375.98	0.24	61.02	9.74	62.82
Netherlands	34	0.02	1.65	1.36	0.07	530.93	0.21	52.74	17.50	164.33
Austria	2090	0.03	1.24	1.21	0.08	251.44	0.15	27.92	8.93	73.60
Poland	1623	0.03	1.16	1.17	0.07	209.93	0.17	43.33	38.31	376.04
Portugal	2745	0.03	1.49	1.36	0.09	295.27	0.14	35.48	10.31	57.56
Slovenia	92	0.03	1.29	1.25	0.08	342.80	0.25	84.81	2.11	15.85
Slovakia	653	0.03	1.33	1.23	0.09	399.04	0.11	27.6	5.46	37.05
Finland	11 600	0.04	1.52	1.41	0.06	182.71	0.14	34.49	5.53	47.78
Sweden	12 079	0.03	1.48	1.51	0.07	37.29	0.07	45.98	10.38	46.28
Norway	983	0.02	1.52	1.42	0.07	63.52	0.11	40.24	5.39	49.27
Switzerland	92	0.08	1.60	1.74	0.07	178.25	0.20	82.01	8.77	43.41
European Union	N/A	0.03	1.45	1.36	0.08	337.00	0.16	47.54	448.26	3298.24
(EU)										

^a for fossil fuels, non-country specific environmental impacts (EIs) are assumed, taking cradle-to-gate emission data from Ecoinvent [66] for IPCC 2013, global warming potential (GWP) 100a, and direct emissions from burning fuels into account: $e_t^{\text{diesel}} = 0.340 \text{ kg CO}_{2\text{-eq}}/\text{kg}$, $e_t^{\text{gasoline}} = 0.309 \text{ kg CO}_{2\text{-eq}}/\text{kg}$, $e_t^{\text{nat.gas}} = 0.277 \text{ kg CO}_{2\text{-eq}}/\text{kg}$, $e_t^{\text{H}_2} = 2.535 \text{ kg CO}_{2\text{-eq}}/\text{kg}$, b^{**} refers to a future, defossilized electrical grid, with characteristics adapted from Santeccchia [93].

184 **C Supplementary information on the results**

185 **Choice of residential district size**

186 For determining an adequate size of the district to be considered for integration, the performance of
187 conventional mill operation is analyzed with different district sizes, allowing for no conventional heating
188 of the district. The sensitivity analysis reveals that for the assumed heating demands (Table 8), a city
189 size of 170000 inhabitants could theoretically be heated by the mill, given the mill is operating in a
190 conventional mode without fuel production and other additional process units. For the presented study,
191 a district size of 85000 is chosen, to allow for the analysis of trade-offs between the provision of different
192 energy commodities. However, it needs to be noted that the outcomes of the study, specifically the
193 reported expenses or emission reduction potentials per inhabitant, are largely linked to the assumption
194 of district size.

195 **System configurations**

196 The results of optimization for Perspective S with a district size of 85000 inhabitants is presented in Table
197 18. The configurations that are selected by the internal optimization and manually are highlighted in
198 grey.

199 **D Design references**

200 Icons for describing the superstructure development were extracted from Flaticon: www.flaticon.com.

201 **Glossary**

202 **CFB** circulating fluidized bed.

203 **DHN** district heating network.

204 **DME** dimethyl ether.

205 **EI** environmental impact.

206 **ENF** entrained flow.

207 **EU** European Union.

Table 18: Results of system analysis with district size of 85000 capita.

ID	$\eta^{\text{self,electricity}}$	$\eta^{\text{self,transport}}$	$\eta^{\text{self,heating}}$	$\eta^{\text{self,combined}}$	S1	S12	$c^{\text{avoidance}}$	$\Delta\text{EI}/\text{cap}$	$\Delta\text{TOTEX}/\text{cap}$
	%	%	%	%	%	%	USD/t CO_2	kg CO_2	USD
0	41.3	60.1	46.3	51.3	46.4	328.3	9.3	654.4	6.1
1	44.8	9.8	46.9	36.0	18.5	394.9	-52.9	787.3	-41.7
2	44.3	11.1	47.0	36.3	18.7	343.4	-106.2	684.6	-72.7
3	43.3	56.9	44.5	49.5	47.3	300.1	-88.0	598.3	-52.6
4	42.6	69.7	44.0	52.9	51.3	318.1	-84.6	634.2	-53.7
5	44.1	91.1	40.7	57.8	59.1	404.2	25.5	805.8	20.5
6	43.0	58.3	44.4	49.8	47.6	355.2	-81.3	708.0	-57.5
7	42.5	69.4	44.0	52.8	51.2	347.1	-71.7	692.0	-49.6
8	42.4	67.4	44.3	52.4	50.5	289.4	-136.5	576.9	-78.7
9	44.7	50.4	44.0	47.7	45.6	408.6	5.1	814.6	4.1
10	44.8	7.0	46.5	35.0	17.1	444.7	-61.6	886.5	-54.6
11	44.7	9.2	46.7	35.7	18.1	369.0	-68.3	735.7	-50.2
12	44.6	7.0	50.8	37.3	16.7	469.8	-6.2	936.6	-5.8
13	53.8	3.7	40.1	33.7	21.8	496.3	230.4	989.5	227.9
14	82.2	0.2	26.5	29.3	39.1	550.0	920.2	1096.4	1008.9
15	43.5	100.0	40.9	60.5	62.3	434.9	52.6	867.0	45.6
16	43.5	100.0	41.8	60.8	62.7	441.0	72.0	879.2	63.3
17	52.7	100.0	36.9	57.2	69.7	469.0	328.0	935.0	306.7
18	50.5	100.0	38.1	57.9	67.8	464.7	275.9	926.4	255.6
19	82.2	100.0	24.8	47.2	89.3	525.5	1014.7	1047.5	1062.9
20	82.2	100.0	24.8	47.2	89.3	525.5	1024.7	1047.6	1073.5

Table 19: Author acknowledgments of icons from Flaticon.

Icons	Author's website hyper-link
Solar panel icon, electric pole icon, worker icon, boiler icon, paper stack icon, tree icon	Freepik
Bus icon	Hight Quality Icons
Car icon	fjstudio
Electric car icon, truck icon	ksonian
House icon	Kiranshastry
Building icon, power generation icon	Smashicons
Fuel icon	Those Icons
Factory icon	monkik
People icon	Vitaly Gorbachev
Solar panel icon	Khoirul Huda

208 **FICFB** fast internally circulating fluidized bed.

209 **FT** Fischer-Tropsch.

210 **GWP** global warming potential.

211 **LHS** latin hypercube sampling.

212 **LHV** lower heating value.

213 **MEA** monoethanolamine.

214 **MILP** mixed integer linear programming.

215 **SNG** synthetic natural gas.

216 **TSA** time series aggregation.

217 **WGS** water gas shift.

218 References

- 219 [1] J Granacher, TV Nguyen, R Castro-Amoedo, EC McDonald and F Maréchal. “Enhancing biomass
220 utilization by combined pulp and fuel production”. In: *Frontiers in Energy Research* 10 (2022).
- 221 [2] M Kermani, ID Kantor, AS Wallerand, J Granacher, AV Ensinas and F Maréchal. “A Holistic
222 Methodology for Optimizing Industrial Resource Efficiency”. en. In: *Energies* 12.7 (Jan. 2019),
223 p. 1315.
- 224 [3] K Pettersson and S Harvey. “Comparison of black liquor gasification with other pulping biorefinery
225 concepts – Systems analysis of economic performance and CO2 emissions”. In: *Energy*. 7th Biennial
226 International Workshop “Advances in Energy Studies” 37.1 (Jan. 2012), pp. 136–153.
- 227 [4] TN Adams. *Lime kiln principles and operations*. en. Tech. rep. Seattle: Tappi, 2007, p. 15.
- 228 [5] DR Sanchez. *Recausticizing - Principles and Practice*. en. Tech. rep. Orlando, FL: Tappi, 2000,
229 p. 30.
- 230 [6] AdS Castro and LS Figueiredo. “Optimization of lime kilns based on strategies of advanced process
231 control - case study Cenibra”. en. In: *5 th International Colloquium on Eucalyptus Pulp*. Bahia,
232 Brazil, May 2011, p. 10.
- 233 [7] J Gullichsen and CJ Fogelholm. *Chemical Pulping, Part 2*. en. Papermaking science and technology.
234 Fapet Oy, 1999.
- 235 [8] Per Lundqvist. “Mass and energy balances over the lime kiln in a kraft pulp mill”. en. PhD thesis.
236 2009.
- 237 [9] M Gassner, F Vogel, G Heyen and F Maréchal. “Optimal process design for the polygeneration
238 of SNG, power and heat by hydrothermal gasification of waste biomass: Process optimisation for
239 selected substrates”. en. In: *Energy & Environmental Science* 4.5 (Apr. 2011), pp. 1742–1758.
- 240 [10] JA Onwudili and PT Williams. “Hydrothermal reactions of sodium formate and sodium acetate
241 as model intermediate products of the sodium hydroxide-promoted hydrothermal gasification of
242 biomass”. en. In: *Green Chemistry* 12.12 (2010). Number: 12, p. 2214.
- 243 [11] M Magdeldin and M Järvinen. “Supercritical water gasification of Kraft black liquor: Process design,
244 analysis, pulp mill integration and economic evaluation”. en. In: *Applied Energy* 262 (Mar. 2020),
245 p. 114558.

- 246 [12] M Schubert, J Aubert, JB Müller and F Vogel. “Continuous salt precipitation and separation from
247 supercritical water. Part 3: Interesting effects in processing type 2 salt mixtures”. en. In: *The Journal*
248 *of Supercritical Fluids* 61 (Jan. 2012), pp. 44–54.
- 249 [13] JS Luterbacher, M Fröling, F Vogel, F Maréchal and JW Tester. “Hydrothermal Gasification of
250 Waste Biomass: Process Design and Life Cycle Assessment”. In: *Environmental Science & Technology*
251 43.5 (Mar. 2009), pp. 1578–1583.
- 252 [14] M Magdeldin, T Kohl and M Järvinen. “Process modeling, synthesis and thermodynamic evaluation
253 of hydrogen production from hydrothermal processing of lipid extracted algae integrated with a
254 downstream reformer conceptual plant”. en. In: *Biofuels* 7.2 (Mar. 2016). Number: 2, pp. 97–116.
- 255 [15] A Mian, AV Ensinas and F Marechal. “Multi-objective optimization of SNG production from mi-
256 croalgae through hydrothermal gasification”. en. In: *Computers & Chemical Engineering* 76 (May
257 2015), pp. 170–183.
- 258 [16] K Özdenkçi, C De Blasio, G Sarwar, K Melin, J Koskinen and V Alopaeus. “Techno-economic fea-
259 sibility of supercritical water gasification of black liquor”. en. In: *Energy* 189 (Dec. 2019), p. 116284.
- 260 [17] C Cao, L Guo, H Jin, W Cao, Y Jia and X Yao. “System analysis of pulping process coupled with
261 supercritical water gasification of black liquor for combined hydrogen, heat and power production”.
262 In: *Energy* 132 (May 2017).
- 263 [18] AM Ribeiro, CA Grande, FV Lopes, JM Loureiro and AE Rodrigues. “A parametric study of
264 layered bed PSA for hydrogen purification”. en. In: *Chemical Engineering Science* 63.21 (Nov.
265 2008). Number: 21, pp. 5258–5273.
- 266 [19] M Magdeldin, T Kohl, C De Blasio, M Järvinen, S Won Park and R Giudici. “The BioSCWG Pro-
267 ject: Understanding the Trade-Offs in the Process and Thermal Design of Hydrogen and Synthetic
268 Natural Gas Production”. en. In: *Energies* 9.10 (Oct. 2016). Number: 10, p. 838.
- 269 [20] D Chiche and JM Schweitzer. “Investigation of competitive COS and HCN hydrolysis reactions
270 upon an industrial catalyst: Langmuir-Hinshelwood kinetics modeling”. en. In: *Applied Catalysis B:*
271 *Environmental* 205 (May 2017), pp. 189–200.
- 272 [21] Markus Lesemann. *RTI and Eastman Chemical Demonstrate Warm-Temperature Syngas Cleanup*
273 *Technology*. en. Tech. rep. RTI International, 2013, p. 4.
- 274 [22] DL Denton, R Gupta, M Lesemann and B Turk. *RTI Warm Syngas Cleanup Technology Demon-*
275 *stration*. en. 2016.

- 276 [23] AD Celebi, S Sharma, AV Ensinas and F Maréchal. “Next generation cogeneration system for
277 industry – Combined heat and fuel plant using biomass resources”. In: *Chemical Engineering Science*
278 204 (Aug. 2019), pp. 59–75.
- 279 [24] E Peduzzi. “Biomass To Liquids”. en. PhD thesis. Switzerland: EPFL, 2015.
- 280 [25] M Gassner and F Maréchal. “Thermo-economic process model for thermochemical production of
281 Synthetic Natural Gas (SNG) from lignocellulosic biomass”. en. In: *Biomass and Bioenergy* 33.11
282 (Nov. 2009), pp. 1587–1604.
- 283 [26] L Tock, M Gassner and F Maréchal. “Thermochemical production of liquid fuels from biomass:
284 Thermo-economic modeling, process design and process integration analysis”. en. In: *Biomass and*
285 *Bioenergy* 34.12 (2010), pp. 1838–1854.
- 286 [27] S Heyne and S Harvey. “Impact of choice of CO₂ separation technology on thermo-economic per-
287 formance of Bio-SNG production processes”. en. In: *International Journal of Energy Research* 38.3
288 (2014), pp. 299–318.
- 289 [28] G Matute, J Yusta and L Correas. “Techno-economic modelling of water electrolyzers in the range
290 of several MW to provide grid services while generating hydrogen for different applications: A case
291 study in Spain applied to mobility with FCEVs”. en. In: *International Journal of Hydrogen Energy*
292 44.33 (July 2019). Number: 33, pp. 17431–17442.
- 293 [29] X Zhang, Y Song, G Wang and X Bao. “Co-electrolysis of CO₂ and H₂O in high-temperature solid
294 oxide electrolysis cells: Recent advance in cathodes”. en. In: *Journal of Energy Chemistry. CO₂*
295 *Capture Storage and Utilization* 26.5 (Sept. 2017), pp. 839–853.
- 296 [30] R Suciú, P Stadler, A Ashouri and F Maréchal. “Towards energy-autonomous cities using CO₂
297 networks and Power to Gas storage”. In: *Proceedings of ECOS 2016*. Postoroz, Slovenia, 2016.
- 298 [31] H Ostovari, A Sternberg and A Bardow. “Rock ‘n’ use of CO₂: carbon footprint of carbon capture
299 and utilization by mineralization”. en. In: *Sustainable Energy & Fuels* 4.9 (2020). Publisher: Royal
300 Society of Chemistry, pp. 4482–4496.
- 301 [32] AC Spínola, CT Pinheiro, AGM Ferreira and LM Gando-Ferreira. “Mineral carbonation of a pulp
302 and paper industry waste for CO₂ sequestration”. en. In: *Process Safety and Environmental Pro-*
303 *tection* 148 (Apr. 2021), pp. 968–979.

- 304 [33] R Castro-Amoedo, J Granacher, MA Daher and F Marechal. “On the role of system integration of
305 carbon capture and mineralization in achieving net-negative emissions in industrial sectors”. en. In:
306 *Energy & Environmental Science* (July 2023). Publisher: The Royal Society of Chemistry.
- 307 [34] J Sipilä, S Teir and R Zevenhoven. *Carbon Dioxide Sequestration by Mineral Carbonation: Literature
308 Review Update 2005–2007*. Tech. rep. Abo Akademi University, Jan. 2008.
- 309 [35] European Technology Platform for Zero Emissions in Fossil Fuel Power Plants. *The costs of CO2
310 transport: post-demonstration CCS in the EU*. en-AU. Tech. rep. Brussels, Belgium, 2011.
- 311 [36] RA Suci. “Fifth generation district energy systems for low carbon cities”. eng. PhD thesis. Lausanne:
312 EPFL, 2019.
- 313 [37] F Belfiore. “District heating and cooling systems to integrate renewable energy in urban areas”.
314 eng. PhD thesis. Lausanne: EPFL, 2021.
- 315 [38] V Masatin, E Latõšev and A Volkova. “Evaluation Factor for District Heating Network Heat Loss
316 with Respect to Network Geometry”. en. In: *Energy Procedia*. International Scientific Conference
317 “Environmental and Climate Technologies”, CONECT 2015 95 (Sept. 2016), pp. 279–285.
- 318 [39] S Henchoz, C Weber, F Maréchal and D Favrat. “Performance and profitability perspectives of
319 a CO2 based district energy network in Geneva’s City Centre”. en. In: *Energy* 85 (June 2015),
320 pp. 221–235.
- 321 [40] P Stadler, L Girardin, A Ashouri and F Maréchal. “Contribution of Model Predictive Control in the
322 Integration of Renewable Energy Sources within the Built Environment”. In: *Frontiers in Energy
323 Research* 6 (2018).
- 324 [41] L Girardin, F Marechal, M Dubuis, N Calame-Darbellay and D Favrat. “EnerGis: A geographical
325 information based system for the evaluation of integrated energy conversion systems in urban areas”.
326 en. In: *Energy*. ECOS 2008 35.2 (Feb. 2010), pp. 830–840.
- 327 [42] Federal Statistical Office. *Energy sector*. en. 2022.
- 328 [43] EK Vakkilainen. “Steam Generation from Biomass, chapter 3: Boiler process”. en. In: *Steam Gen-
329 eration from Biomass*. Ed. by EK Vakkilainen. Butterworth-Heinemann, Jan. 2017, pp. 57–86.
- 330 [44] A Ashouri. “Simultaneous Design and Control of Energy Systems”. en. Accepted: 2017-10-04T08:17:55Z.
331 Doctoral Thesis. ETH Zurich, 2014.
- 332 [45] T Elghozi. *How to calculate the indicators for the transport sector*. en. 2021.

- 333 [46] L Calearo, M Marinelli and C Ziras. “A review of data sources for electric vehicle integration
334 studies”. en. In: *Renewable and Sustainable Energy Reviews* 151 (Nov. 2021), p. 111518.
- 335 [47] International Energy Agency. *Vehicle fuel economy in major markets 2005-2019*. en. Tech. rep.
336 International Energy Agency, 2021.
- 337 [48] J Szargut, DR Morris and FR Steward. *Exergy analysis of thermal, chemical, and metallurgical
338 processes*. English. Berlin, Heidelberg: Springer, 1988.
- 339 [49] Eurostat. *Road traffic by type of vehicle*. 2022.
- 340 [50] International Energy Agency. *Net Zero by 2050 - A Roadmap for the Global Energy Sector*. en.
341 Tech. rep. International Energy Agency, 2021, p. 224.
- 342 [51] L Middelhaue. “On the role of districts as renewable energy hubs”. eng. PhD thesis. Lausanne:
343 EPFL, 2022.
- 344 [52] PM Stadler. “Model-based sizing of building energy systems with renewable sources”. eng. PhD
345 thesis. Lausanne: EPFL, 2019.
- 346 [53] Cedric Terrier, Luise Middelhaue and François Maréchal. “Potential of electric mobility as service
347 to the grid in renewable energy hubs”. In: *Proceedings of ECOS 2022 - The 35th International
348 Conference on Efficiency, Cost, Optimization, Simulation and Environmental Impact of Energy
349 Systems*. Vol. 35. Copenhagen, Denmark, 2022.
- 350 [54] Eurostat. *Territorialised road freight transport, by transport coverage – annual data*. 2022.
- 351 [55] M Gassner and F Maréchal. “Methodology for the optimal thermo-economic, multi-objective design
352 of thermochemical fuel production from biomass”. In: *Computers & Chemical Engineering*. Selec-
353 ted Papers from the 17th European Symposium on Computer Aided Process Engineering held in
354 Bucharest, Romania, May 2007 33.3 (Mar. 2009), pp. 769–781.
- 355 [56] I Kantor, JL Robineau, H Bütün and F Maréchal. “A Mixed-Integer Linear Programming Formula-
356 tion for Optimizing Multi-Scale Material and Energy Integration”. In: *Frontiers in Energy Research*
357 8 (2020), p. 49.
- 358 [57] R Castro-Amoedo, N Morisod, J Granacher and F Maréchal. “The Role of Biowaste: A Multi-
359 Objective Optimization Platform for Combined Heat, Power and Fuel”. In: *Frontiers in Energy
360 Research* 9 (2021), p. 417.

- 361 [58] F Marechal and B Kalitventzeff. “Process integration: Selection of the optimal utility system”. In:
362 *Computers & Chemical Engineering*. European Symposium on Computer Aided Process Engineering-
363 8 22 (Mar. 1998), S149–S156.
- 364 [59] B Linnhoff and E Hindmarsh. “The pinch design method for heat exchanger networks”. In: *Chemical*
365 *Engineering Science* 38.5 (1983). 00000, pp. 745–763.
- 366 [60] M Kermani, Z Perin-Levasseur, M Benali, L Savulescu and F Marechal. “A novel MILP approach for
367 simultaneous optimization of water and energy: Application to a Canadian softwood Kraft pulping
368 mill”. en. In: *Computers & Chemical Engineering* 102 (2017), pp. 238–257.
- 369 [61] M Hoffmann, L Kotzur, D Stolten and M Robinius. “A Review on Time Series Aggregation Methods
370 for Energy System Models”. en. In: *Energies* 13.3 (Jan. 2020). Number: 3 Publisher: Multidiscip-
371 linary Digital Publishing Institute, p. 641.
- 372 [62] T Schütz, MH Schraven, M Fuchs, P Remmen and D Müller. “Comparison of clustering algorithms
373 for the selection of typical demand days for energy system synthesis”. en. In: *Renewable Energy* 129
374 (Dec. 2018), pp. 570–582.
- 375 [63] L Middelhaue, N Ljubic, J Granacher, L Girardin and F Maréchal. “Data reduction for mixed
376 integer linear programming in complex energy systems”. In: *Proceedings of ECOS 2021*. 2021.
- 377 [64] N Baumgärtner, B Bahl, M Hennen and A Bardow. “RiSES3: Rigorous Synthesis of Energy Supply
378 and Storage Systems via time-series relaxation and aggregation”. en. In: *Computers & Chemical*
379 *Engineering* 127 (Aug. 2019), pp. 127–139.
- 380 [65] B Bahl, A Kümpel, H Seele, M Lampe and A Bardow. “Time-series aggregation for synthesis
381 problems by bounding error in the objective function”. In: *Energy* 135 (2017), pp. 900–912.
- 382 [66] G Wernet, C Bauer, B Steubing, J Reinhard, E Moreno-Ruiz and B Weidema. “Theecoinvent
383 database version 3 (part I): overview and methodology”. en. In: *The International Journal of Life*
384 *Cycle Assessment* 21.9 (Sept. 2016), pp. 1218–1230.
- 385 [67] Food and Agriculture Organization of the United Nations. *Forest Products Annual Market Review,*
386 *2018-2019*. Tech. rep. ECE/TIM/SP/48. ISBN: 978-92-1-117218-8. United Nations, 2019.
- 387 [68] Index Mundi. *Wood Pulp - Monthly Price*. 2022.
- 388 [69] Eurostat. *Electricity prices for non-household consumers - bi-annual data*. 2022.
- 389 [70] Eurostat. *Gas prices for non-household consumers - bi-annual data*. 2022.

- 390 [71] I Landälv, K Maniatis, Evd Heuvel, S Kalligeros and L Waldheim. *Building up the future, cost*
391 *of biofuel : sub group on advanced biofuels : sustainable transport forum*. en. Brussels, Belgium:
392 Publications Office of the European Union, June 2018.
- 393 [72] Methanex. *Methanex Monthly Average Regional Posted Contract Price History*. 2021.
- 394 [73] P Zeman, V Hönig, P Procházka and J Mařík. “Dimethyl ether as a renewable fuel for diesel
395 engines”. en. In: *Agronomy Research* 15 (2017).
- 396 [74] J Gorre, F Ortloff and C van Leeuwen. “Production costs for synthetic methane in 2030 and 2050
397 of an optimized Power-to-Gas plant with intermediate hydrogen storage”. en. In: *Applied Energy*
398 253 (Nov. 2019), p. 113594.
- 399 [75] International Energy Agency. *The Future of Hydrogen*. en-GB. Technology Report. Paris, France:
400 International Energy Agency, June 2019, p. 203.
- 401 [76] Index Mundi. *Lime Prices In The United States, By Type*. 2022.
- 402 [77] European Association of Public Water Operators. *Water affordability*. Tech. rep. Brussels: European
403 Association of Public Water Operators, 2016.
- 404 [78] Valmet. *The modern white liquor plant*. Tech. rep. Valmet, 2017.
- 405 [79] International Energy Agency. *Special Report on Carbon Capture Utilisation and Storage: CCUS in*
406 *clean energy transitions*. en. Tech. rep. International Energy Agency, 2020, p. 174.
- 407 [80] WJ Schmelz, G Hochman and KG Miller. “Total cost of carbon capture and storage implemented at
408 a regional scale: northeastern and midwestern United States”. In: *Interface Focus* 10.5 (Oct. 2020),
409 p. 20190065.
- 410 [81] G Gullberg, F Ericson and M Eck. *The French District Heating Market – Overview, Opportunities*
411 *and Challenges*. en. Tech. rep. Swedish Energy Agency, 2019, p. 33.
- 412 [82] European Commission. *Weekly Oil Bulletin*. en. 2022.
- 413 [83] Entsoe. *European association for the cooperation of transmission system operators for electricity*.
414 en-us. 2022.
- 415 [84] Macrotrends LLC. *WTI Crude Oil Prices - 10 Year Daily Chart — MacroTrends*. 2023.
- 416 [85] GA Buchner, AW Zimmermann, AE Hohgräve and R Schomäcker. “Techno-economic Assessment
417 Framework for the Chemical Industry—Based on Technology Readiness Levels”. In: *Industrial &*
418 *Engineering Chemistry Research* 57.25 (June 2018), pp. 8502–8517.

- 419 [86] US Energy Information Administration. *Factors affecting natural gas prices - U.S. Energy Inform-*
420 *ation Administration (EIA)*. 2022.
- 421 [87] C Bencivenga, G Sargenti and RL D’Ecclesia. “Energy markets: crucial relationship between prices”.
422 en. In: *Mathematical and Statistical Methods for Actuarial Sciences and Finance*. Ed. by M Corazza
423 and C Pizzi. Milano: Springer Milan, 2010, pp. 23–32.
- 424 [88] U Albrecht, M Altmann, J Zerhusen, T Rakhsa, P Maio, A Beaudet, P Trucco, C Egenhofer, A
425 Behrens, J Teusch, J Wiczorkiewicz, F Genoese and G Maisonnier. *The impact of the oil price on*
426 *EU energy prices*. Tech. rep. Policy Department European Parliament, 2014.
- 427 [89] T Kanamura. “A model of price correlations between clean energy indices and energy commodities”.
428 In: *Journal of Sustainable Finance & Investment* 12.2 (Apr. 2022), pp. 319–359.
- 429 [90] MU Rehman. “Dynamic correlation pattern amongst alternative energy market for diversification
430 opportunities”. In: *Journal of Economic Structures* 9.1 (Feb. 2020), p. 16.
- 431 [91] N Lange. “Correlation in Energy Markets”. en. PhD thesis. Frederiksberg: Copenhagen Business
432 School, 2017.
- 433 [92] Eurostats. *Pulp, paper and paperboard*. 2022.
- 434 [93] A Santecchia. “Enabling renewable Europe through optimal design and operation”. eng. PhD thesis.
435 Lausanne: EPFL, 2022.
- 436 [94] Eurostat. *Population and employment*. 2023.
- 437 [95] European Environment Agency. *EEA greenhouse gases*. en. Dashboard (Tableau). 2022.